Pramana – J. Phys. (2022) 96:96
https://doi.org/10.1007/s12043-022-02347-6

Photon-induced low-energy nuclear reactions

PANKAJ JAIN[1],*, ANKIT KUMAR[1], RAJ PALA[2] and K P RAJEEV[1]

[1]Physics Department, Indian Institute of Technology, Kanpur 208 016, India
[2]Department of Chemical Engineering, Indian Institute of Technology, Kanpur 208 016, India
*Corresponding author. E-mail: pkjain@iitk.ac.in

MS received 1 September 2020; revised 1 January 2022; accepted 18 January 2022

Abstract. We propose a new mechanism for inducing low-energy nuclear reactions (LENRs). The process is initiated by a perturbation which we assumed to be caused by absorption or emission of a photon. Due to the electromagnetic perturbation, the initial two-body nuclear state forms an intermediate state to make a transition into the final nuclear state through the action of another perturbation. In the present paper, we take the second perturbation to be also electromagnetic. We need to sum over all energies of the intermediate state. Since the upper limit on this sum is infinity it is possible to get contributions from very high energies for which the barrier penetration factor is not too small. By considering a specific reaction, we determine the conditions under which this mechanism may lead to significantly enhanced reaction rates. We find that the mechanism leads to very small cross-sections in free space. However, in a condensed medium, there exist several possibilities leading to enhanced cross-sections, which may lead to observable reaction rates even at relatively low energies. Hence we argue that LENRs are possible and provide a theoretical set-up which may explain some of the experimental claims in this field.

Keywords. Low-energy nuclear reactions; nuclear electromagnetic transitions; Coulomb barrier; nuclear fusion with two-photon emission.

PACS Nos 24; 25.10.+s; 14.70.Bh

1. Introduction

The phenomenon of low-energy nuclear reactions (LENRs) has now been studied for many decades. The original results presented in [1,2] were quickly dismissed since many of the follow-up experiments could not reproduce them. Several experiments did find confirmation of the results while others disagreed. A major reason for the dismissal was that the phenomenon was thought to be theoretically impossible [3,4]. However, both experimental and theoretical research in this field has continued over the years. A useful summary is provided in [5–17] and in the collection of articles in ref. [18]. Several theoretical proposals also exist [19–28]. Many theoretical papers are devoted to study the screening due to electrons in a condensed medium [20,29,30]. A detailed study of screening can be seen in [20] with the conclusion that by itself it is unable to explain the enhanced cross-sections even in the energy range of 1 keV [19]. Electroweak intereactions have also been invoked to explain the phenomenon [27]. Furthermore, it has been suggested that the incident particle may be in a superposition of several states and due to destructive interference, the reflection coefficient becomes significantly smaller than unity leading to considerable enhancement in transmission [22]. It has also been proposed that the nuclear particles may form clusters due to enhanced electron screening which may lead to smaller Coulomb barrier [23]. However, the LENR phenomena is still not understood theoretically. A critical review of several theoretical proposals is given in [31].

Experimentally, it is quite clear that there is indeed an enhancement of cross-sections at low energies [19, 20,32–38]. Furthermore, there exists some evidence that such low-energy experiments produce γ-rays and other particles which can only be produced by nuclear reactions [39–42]. It has been argued that the experimental data are better characterised in terms of production of nuclear particles rather than excess heat [43]. We also point out that experiments in the energy range of order of a few keV have consistently shown enhanced cross-sections [37,38]. Some of these experiments involve a beam of high-energy deuteron ions impinging on a solid medium [37]. The lower energy experiments use electrolysis at some suitably chosen potential differences.

Published online: 05 May 2022

The community has slowly come to an agreement that the nuclear fusion cross-sections in this energy regime are much higher than theoretically expected and the ratio of experimental to theoretically predicted cross-sections increases rapidly with decrease in energy.

We point out that there exist well-known situations in which a particle can tunnel through a high potential barrier with rather high probability. We consider a textbook example of a double hump potential (see page 129 of [44], third edition). Here we assume that the potential barrier is much larger than the energy of the incident particle. Using the WKB approximation, one finds that although the transmission for such a potential is generally small, there exist some special values of energy for which the transmission can be very large. It is not clear whether such a mechanism is really realised in nuclear fusion reactions in condensed medium [31]. Here we use it only to illustrate that high potential does not always mean low transmission. It is also well known that the nuclear fusion rates are rather large if the reaction proceeds by resonance. This arises when the energy of the incident particle is equal or closer to one of the nuclear states. In the present paper, however, we shall not consider resonant reactions.

We are interested in explaining the phenomena of LENRs, the energies being of order eV. In this paper, we propose a new process which may be relevant for LENRs. In this case, the reaction proceeds by an electromagnetic perturbation in the initial state. This perturbation may be in the form of a real photon or a virtual photon. Here we assume it to be a real photon which may be absorbed or emitted. The perturbation leads to the formation of an intermediate state which can be expressed as a superposition of all eigenstates of the unperturbed Hamiltonian. Each of these eigenstates then can contribute to the fusion process. As prescribed by the uncertainty principle, each of these states can exist for a short time interval during which they can undergo fusion. As there is no restriction on the energy of these states, it is possible that the barrier penetration factor may not lead to a strong suppression. Here, we develop the formalism for such reactions, which proceed at second order in the time-dependent perturbation theory, and provide estimates for some simple cases.

Ideas similar to ours have been proposed earlier. For example, Kálmán and Keszthelyi [24] proposed that the fusion process is assisted by the presence of a medium particle. The Coulomb interaction between the medium nucleus and the particles undergoing fusion act as the perturbation. We also assume an electromagnetic perturbation. However, in our case it leads to either an emission or an absorption of a photon. To the best of our knowledge, this process has not been discussed in the literature in this context. As we shall see, the calculation is very useful since it highlights several pitfalls that might be encountered in this approach and may suggest possible ways in which these can be overcome.

In our analysis we shall focus on the reaction

$$^1\mathrm{H} + {}^2\mathrm{H} + \gamma(\omega_i) \rightarrow {}^3\mathrm{He} + \gamma(\omega_f). \tag{1}$$

This involves fusion of hydrogen with deuteron to form ^{3}He induced by an incident flux of photons. In contrast, the standard reaction can be written as

$$^1\mathrm{H} + {}^2\mathrm{H} \rightarrow {}^3\mathrm{He} + \gamma(\omega_f). \tag{2}$$

A reaction, somewhat related to eq. (1),

$$^1\mathrm{H} + {}^2\mathrm{H} \rightarrow {}^3\mathrm{He} + \gamma(\omega_1) + \gamma(\omega_2)\,, \tag{3}$$

has also been studied in a follow-up paper by our group [45]. This involves emission of two photons in contrast to one photon in eq. (2). The processes in eqs (1) and (3) proceed at second order in perturbation theory in contrast to the standard reaction which gets dominant contribution at first order. Our main motivation for studying these reactions is that these provide the simplest system for studying low-energy nuclear reactions. If this phenomenon is real, it is likely to be very complex and other reactions may be taking place besides those described above. However, these provide a good starting point for a theoretical analysis. These reactions are also interesting since they predict a clear experimental signal of photon emission, which can be tested cleanly.

Let us now briefly review the standard fusion rate calculations [46–50]. Consider the nuclear fusion reaction in which a light nucleus a is incident on the target nucleus B,

$$a + B \rightarrow C + d. \tag{4}$$

Here C is the final nucleus and d is another particle, which may be a photon, neutron or a pair of particles, such as a neutrino and a positron. We use the centre of mass and relative coordinates and convert the initial two-body system into an effective one-body problem by introducing the concept of reduced mass. The particle a may be a proton or a deuteron or some other light nuclei. We assume that the kinetic energy of the initial state is E when the two particles are at large distances from one another. Let Z_1 and Z_2 be the atomic numbers of the two initial state nuclei and A_1 and A_2 be their atomic mass numbers. We consider the non-resonant case in which there is no nuclear bound state with energy equal to the incident two-particle energy. The important factors which contribute to the reaction rate are the tunnelling probability and rate of decay of this state into a nuclear state by the emission of particle d. The cross-section for this process may be expressed as [46,47]

$$\sigma(E) = \frac{S(E)}{E}\, B(E), \tag{5}$$

where

$$B(E) = \exp(-b/\sqrt{E}) \tag{6}$$

and b is a constant. If we ignore screening, the factor b is given by [46]

$$b = 31.28 Z_1 Z_2 \sqrt{A}\,\mathrm{keV}^{1/2}, \tag{7}$$

where $A = A_1 A_2/(A_1 + A_2)$ is the reduced atomic mass. Here the exponential factor represents the probability for barrier penetration and the remaining factors depend on the amplitude for production of particle d. Hence, for the case of photon production, the factor $S(E)$ will depend on the electromagnetic coupling. For the case of non-resonant scattering, $S(E)$ is a slowly varying function of E. For the case of no screening, i.e. just Coulomb repulsion between two nuclei, the barrier penetration can be shown to take the form given in the exponent in eq. (6) to a very good approximation [46]. In general, when screening due to electrons is taken into account, the form may be somewhat more complicated. The screening effects can, however, be incorporated approximately by adding a screening energy E_s to the energy factor E in the exponent in eq. (6).

In §2 we review the calculation of the basic fusion process given in eq. (2). In §3, we analyse the photon-induced process given in eq. (1) and determine the formula for the reaction rate. In §4 we estimate the reaction rate both in free space and in condensed medium. We also use the results of [45] to compute the rate of the two-photon emission reaction, eq. (3), and discuss conditions under which we may get observable effects.

2. Standard fusion process

The fusion reaction typically involves emission of some particle, such as a photon, a light nucleus or a pair of particles such as, a positron and a neutrino. Hence besides involving strong interactions, it may also involve electromagnetic and/or weak interactions. Here we briefly review the calculation of a fusion reaction rate. The main purpose is to validate our potential model, which will be used in the next section to compute our proposed reaction. To be specific, we shall focus on an electromagnetic transition and consider the reaction in eq. (2), i.e. fusion of a proton and a deuteron to form a helium(3) with the emission of a photon. In this work, we shall use atomic units.

Let the initial state two-body wave function be denoted by $|i\rangle$. We assume that the two particles are free initially. The reaction rate will involve the overlap of this wave function with the ^{3}He wave function which will depend on the quantum tunnelling amplitude. The two nuclei in the initial state are treated as an equivalent one particle by introducing the concept of reduced mass. The electrons surrounding the nuclei, which may be either bound or free, modify the effective potential experienced by the two nuclei, i.e. lead to screening of the Coulomb potential. The Hamiltonian of the system can be written as

$$H = H_0 + H_I, \tag{8}$$

where H_0 is the unperturbed Hamiltonian and H_I is the time-dependent perturbation. The unperturbed Hamiltonian is given by

$$H_0 = K_1 + K_2 + \mathcal{V}(r), \tag{9}$$

where K_1 and K_2 are the kinetic energies of the two nuclei and $\mathcal{V}(r)$ is the effective potential. We express H_0 in terms of the centre of mass and relative coordinates and ignore the centre of mass motion. The effective potential $\mathcal{V}(r)$ is obtained after integrating over the contributions from electrons and hence contains the screening potential as well as the nuclear potential. We represent it as

$$\mathcal{V}(r) = \frac{Z_1 Z_2 e^2}{r} \mathrm{e}^{-r/r_0} + V_n, \tag{10}$$

where r_0 is the screening length which we set equal to Bohr radius and the nuclear potential V_n is taken to be of form

$$V_n = -V_0 \mathrm{e}^{-r^2/R^2}. \tag{11}$$

We set the parameters $V_0 = 55$ and $R = 1.81$ fm. This leads to ^{3}He ground state binding energy of 5.49 MeV [45], which is in agreement with the data.

The reaction then proceeds by the emission or absorption of a photon which at leading order can be computed by considering the following time-dependent perturbation (see, for example [44,51]):

$$H_I(t) = -\frac{Z_1 e}{c m_1} \vec{A}(\vec{r}_1, t) \cdot \vec{p} + \frac{Z_2 e}{c m_2} \vec{A}(\vec{r}_2, t) \cdot \vec{p} + \frac{e\hbar g_p}{2 m_p c} \vec{\sigma} \cdot \vec{B} + \cdots, \tag{12}$$

where $\vec{A}$ is the vector potential, Z_1, m_1 and $\vec{r}_1$ are the atomic number, mass and position vector of ^{1}H and Z_2, m_2 and $\vec{r}_2$ the corresponding variables for ^{2}H. Here we have set $\vec{p}_1 = -\vec{p}_2 = \vec{p}$. We have also included the contribution of magnetic moment due to the proton. This is the third term on the right-hand side, with σ_i are the Pauli matrices, $\vec{B} = \vec{\nabla} \times \vec{A}$ is the magnetic field, g_p is the proton g factor and m_p is the proton mass. Its contribution is significant and has been discussed in [45]. In the present paper, we shall not include its contribution for the calculation of rate in the presence of initial flux

of photons. However, in §4.3, we shall use the results of [45], which include this term, to compute the rate of two-photon emission process. We have

$$\vec{A}(\vec{r},t) = \frac{1}{\sqrt{V}}\sum_{\vec{k}}\sum_{\beta} c\sqrt{\frac{\hbar}{2\omega}}[a_{\vec{k},\beta}(t)\vec{\epsilon}_\beta e^{i\vec{k}\cdot\vec{r}} + a^{\dagger}_{\vec{k},\beta}(t)\vec{\epsilon}_\beta e^{-i\vec{k}\cdot\vec{r}}]. \tag{13}$$

We need to compute the transition amplitude, given by

$$\langle f|T(t_0,t)|i\rangle = \left(-\frac{i}{\hbar}\right)\int_{t_0}^{t} dt'\langle f|H_I(t')|i\rangle e^{i(E_f-E_i)t'/\hbar}. \tag{14}$$

It is implicitly assumed that there also exists a photon of frequency ω_f and wave vector $\vec{k}_f$ in the final state. We have not explicitly shown this in the equation above. Inserting the vector potential and acting with the creation operator, we obtain

$$\langle f|T(t_0,t)|i\rangle = \frac{ie\xi}{\hbar\mu}\sqrt{\frac{\hbar}{2\omega_f V}}\int_{t_0}^{t} dt'\langle f|\vec{\epsilon}_\beta\cdot\vec{p}\ |i\rangle e^{i(E_f-E_i+\hbar\omega_f)t'/\hbar}, \tag{15}$$

where $V = L^3$ is the quantisation volume, $\vec{\epsilon}_\beta$ is the photon polarisation vector and E_i and E_f are the energies of the initial and final states respectively. The variable μ is the reduced mass of the two-particle system and ξ is given by

$$\xi = \frac{Z_1m_2 - Z_2m_1}{M}, \tag{16}$$

where $M = m_1 + m_2$. Here we have made the approximation $e^{-i\vec{k}_f\cdot\vec{r}} \approx 1$. This approximation is expected to be valid in the present case since the final-state wave function gets dominant contribution only over nuclear length scales. In our case, $Z_1 = Z_2 = 1$ and hence $\xi = 1/3$. The final state is the ground state of ^{3}He which has spin 1/2 and zero orbital angular momentum. We take the initial state also to be $S = 1/2$ along with $l = 1$. This leads to $j = 3/2$ and 1/2. Here we shall only consider the state $j = 3/2$, $j_z = 3/2$ which is sufficient for our analysis. Including the contribution of other states will only change our results by a factor of order unity and will have no effect on our conclusions. We point out that in the next section we shall perform a complete calculation for the second-order process.

Next, we perform the time integral and take the limit $t_0 \to -\infty$ and $t \to \infty$ to obtain

$$|\langle f|T(t_0,t)|i\rangle|^2 = \frac{e^2\xi^2\pi\,\Delta T}{\mu^2\omega_f V} \times \delta(E_f - E_i + \hbar\omega_f)|\langle f|\vec{\epsilon}_\beta\cdot\vec{p}\ |i\rangle|^2, \tag{17}$$

where $\Delta T = t - t_0$ is the total time. Let ρ_γ be the density of photon states for emission into solid angle $d\Omega$, given by

$$\rho_\gamma = \frac{V\omega_f^2}{(2\pi)^3}\frac{d\Omega}{\hbar c^3}. \tag{18}$$

Using this and integrating over $E_{\gamma f} = \hbar\omega_f$, we obtain the transition probability per unit time $dP_{d\Omega}/dt$ for solid angle $d\Omega$. It is given by

$$\frac{dP_{d\Omega}}{dt} = \int dE_{\gamma f}\rho_\gamma\frac{|\langle f|T(t_0,t)|i\rangle|^2}{\Delta T}. \tag{19}$$

Here we have ignored the small nuclear recoil. The transition probability dP/dt integrated over solid angle can then be expressed as

$$\frac{dP}{dt} = \frac{e^2\xi^2\omega_f}{8\pi^2\hbar c^3\mu^2}\int d\Omega\sum_{\beta}|\langle f|\vec{\epsilon}_\beta\cdot\vec{p}\ |i\rangle|^2, \tag{20}$$

where we have summed over the final-state polarisations. It is convenient to replace the operator $\vec{p}$ by using

$$\vec{p} = i\mu[H_0,\vec{r}\ ]/\hbar. \tag{21}$$

The matrix element can then be expressed as

$$\langle f|\vec{\epsilon}_\beta\cdot\vec{p}\ |i\rangle = \frac{i\mu}{\hbar}(E_f - E_i)\langle f|\vec{\epsilon}_\beta\cdot\vec{r}\ |i\rangle. \tag{22}$$

We next perform the angular integration in eq. (20). We point out that we are considering a dipole transition from the initial state $l = 1$ to the final state $l' = 0$. After summing over photon polarisations and performing the angular integral in eq. (20), we obtain,

$$\frac{dP}{dt} = \frac{8\pi\alpha\xi^2\omega_f}{3\hbar^2c^2}(E_f - E_i)^2\ |I_{fi}|^2, \tag{23}$$

where $\alpha = e^2/(4\pi\hbar c)$, I_{fi} is the integral over the radial wave functions, $R_f(r)$ and $R_i(r)$

$$I_{fi} = \int_0^\infty dr\, r^3 R_f^*(r)R_i(r). \tag{24}$$

Here we have normalised the initial state to a plane wave.

To obtain the cross-section for the process, we divide dP/dt by the number N_2 of target particles in volume V and the incident flux $F(E) = n_1v$, where v is the relative velocity and n_1 is the number density of incident particles. Here we assume that the incident wave, corresponding to the initial state nuclei, is a plane wave normalised over a volume $V = L^3$. The possibility that a wave packet can lead to enhanced tunnelling has been suggested in [52]. However in the present paper, we restrict our analysis to a plane wave. The cross-section can be expressed as

$$\sigma = \frac{1}{N_2F(E)}\frac{dP}{dt}. \tag{25}$$

The factors involving the length parameter L would cancel the normalisation of the wave function to give the final observable cross-section σ. We have chosen a normalisation such that $N_2 = 1$ and $F(E_i) = v/V$, where $v = \sqrt{2E_i/\mu}$ is the relative velocity between the two particles. We may express the cross-section in terms of the standard expression $\sigma = S(E_i)B(E_i)/E_i$ (see eq. (5)). Here $S(E_i)$ is assumed to be a slowly varying function of E_i. Its value at $E_i = 0$ for the process in eq. (2) is given by $S(0) = 2.5 \times 10^{-4}$ keV barn [46].

We next obtain the cross-section using our potential model and compare with the standard formula given in eq. (5). The main purpose of this calculation is to confirm that our potential model is reasonable. For initial energy of $E_i = 10$ keV we obtain 8.3×10^{-9} barns in comparison to 7.8×10^{-9} barns obtained by eq. (5). Hence we obtain fairly good agreement which validates our choice of the potential.

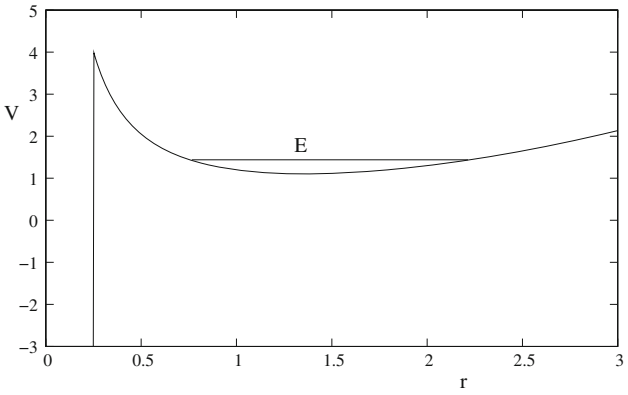

Figure 1. A schematic representation of the potential experienced by nucleus 1 at energy E inside a medium. The potential is centred at the position of another nucleus (2) in the medium. At very short distances, particle 1 experiences the nuclear force due to particle 2. At large distances, it experiences the screened Coulomb force due to interactions with all particles in the medium. The potential levels off at large distances (not shown in the figure).

3. Photon-induced fusion

In this section, we propose a specific higher-order process which may give a large contribution at low energies inside a medium. The basic idea is that while the standard reaction, given in eq. (2) leads to exponentially small rates at low energies, the related processes, given in eqs (1) and (3) may not be as suppressed. These reactions get dominant contribution at second order in the electromagnetic perturbation. We assume a typical low-energy nuclear reaction [1,53] in a medium which is being driven by some external agent, as an electrochemical reaction. We load the system with a large number of light nuclei, such as protons or deuterons, perhaps through an electrochemical process and hence the system is also constantly changing with time. These particles may become bound to other particles and some may be in quasi-free state inside matter. The potential is shown schematically in figure 1 with the particle being in a bound state at energy E. The potential may be split into two parts: the molecular (or atomic) and the nuclear potential, each of which hosts a tower of states, which may be termed molecular and nuclear states respectively. By molecular potential, we mean the potential energy of two nuclei shielded by electrons when they are far away from one another such that the nuclear interaction is negligible. The nuclear potential refers to the potential experienced by the nuclei when they are within a few Fermi distance from one another. These are illustrated in figure 1 by the potential wells at large and small distances respectively from the origin. The wave functions for these two eigenstates peak in the two respective potential wells and decay rapidly in the adjacent well.

We consider the reaction which involves absorption and emission of a photon (eq. (1)). The process involves three particles in the initial state and would depend on the incident photon flux. We may write the second-order contribution to the transition amplitude as

$$\langle f|T(t_0,t)|i\rangle = \left(-\frac{i}{\hbar}\right)^2 \times \sum_n \int_{t_0}^{t} \mathrm{d}t' \mathrm{e}^{i(E_f-E_n)t'/\hbar} \langle f|H_I(t')|n\rangle \times \int_{t_0}^{t'} \mathrm{d}t'' \mathrm{e}^{i(E_n-E_i)t''/\hbar} \langle n|H_I(t'')|i\rangle \quad (26)$$

with $H_I(t)$ given by eq. (12). We point out that in the present case a photon is present in the initial state also. We take its frequency to be ω_i whereas the frequency of the final-state photon is taken to be ω_f. We obtain two contributions to the amplitude [51]. In one of these, the initial-state photon first gets annihilated and later the final-state photon is emitted. In the second case, the time order of these photons is reversed.

We start by considering the first process. In this amplitude, a photon of frequency ω_i is absorbed, followed by emission of photon of frequency ω_f. Since we need to annihilate the photon in the initial state, the time dependence of $H_I(t'')$ is $\mathrm{e}^{-i\omega_i t''}$. The t'' integral then gives

$$\int_{t_0}^{t'} \mathrm{d}t'' \mathrm{e}^{i(E_n-E_i)t''/\hbar} \langle n|H_I(t'')|i\rangle = -\frac{i\hbar e\xi}{\mu}\sqrt{\frac{\hbar}{2\omega_i V}} \langle n|\vec{\epsilon}_\beta \cdot \vec{p}\,|i\rangle$$

$$\times \frac{e^{i(E_n - E_i - \hbar\omega_i)t'/\hbar} - e^{i(E_n - E_i - \hbar\omega_i)t_0/\hbar}}{E_n - E_i - \hbar\omega_i}. \quad (27)$$

Here we have made the dipole approximation and set $e^{i\vec{k}\cdot\vec{r}} \approx 1$ in the photon field operator. To compute the transition matrix element in eq. (26) we substitute the expression for the integral over t'' given in eq. (27). We see from eq. (27) that it involves two separate terms. The second term depends on the arbitrary parameter t_0 which needs to be set equal to $-\infty$ at the end of the calculation. Since we expect that the perturbation would go to zero as $t_0 \to -\infty$, this term should be set to zero. We next evaluate the transition amplitude (eq. (26)). The transition matrix element can be written as

$$\langle f|T(t,t_0)|i\rangle = i\frac{e^2\xi^2}{2\mu^2 V}\sqrt{\frac{1}{\omega_i\omega_f}}\int_{t_0}^{t} dt' e^{i(E_f - E_i - \hbar\omega_i + \hbar\omega_f)t'/\hbar} \times \sum_n \frac{\langle f|\vec{\epsilon}\,'_{\beta'}\cdot\vec{p}\,|n\rangle\langle n|\vec{\epsilon}_\beta\cdot\vec{p}\,|i\rangle}{E_n - E_i - \hbar\omega_i}. \quad (28)$$

We next compute the second amplitude in which a photon of frequency ω_f is first emitted, followed by the absorption of a photon of frequency ω_i. The energy of the emitted photon is of order 5 MeV. This leads to a rather large magnitude of the photon wave vector and it is not possible to use the dipole approximation $e^{-i\vec{k}\cdot\vec{r}} \approx 1$ in this case. We obtain

$$\langle n|H_I(t'')|i\rangle = \frac{e}{\sqrt{V}}\sum_\beta \sqrt{\frac{\hbar}{2\omega_f}}\langle n| \times \left[-\frac{1}{m_1}e^{i\vec{k}_f\cdot\vec{r}m_2/M} + \frac{1}{m_2}e^{-i\vec{k}_f\cdot\vec{r}m_1/M}\right]\vec{\epsilon}\,'_{\beta'}\cdot\vec{p}\,|i\rangle e^{i\omega_f t''}. \quad (29)$$

Here in the exponents we have replaced $\vec{r}_1$ and $\vec{r}_2$ in terms of the relative variable $\vec{r}$ and the centre of mass variable $\vec{R}_{\rm cm}$ and dropped the dependence on $\vec{R}_{\rm cm}$.

The matrix element on the right-hand side in eq. (29) contains one of the key concepts of our paper. Let us first consider the matrix element $\langle n|\vec{\epsilon}_\beta\cdot\vec{p}|i\rangle$ in eq. (27). In a typical case, we are interested in an initial state of energy of order 10 eV and an intermediate state of high energy of order of a few keV. Hence, this matrix element would involve the overlap of a very rapidly varying wave function with other slowly varying factors. The dominant contribution arises only from very small r values for which the initial state wave function decays rapidly. Hence, this matrix element is highly suppressed. In contrast, the amplitude in eq. (29) has explicit dependence on photon wave vector $\vec{k}_f$. This wave vector is rather large and the amplitude is not confined only to small r values. We find that significant contributions are obtained for intermediate state wave vectors $k_n \sim k_f$. For $E_f \sim 5$ MeV, this leads to effective intermediate state energies of order 10 keV. Hence, this matrix element can take rather large values for $E_n \sim 10$ keV and dominate the reaction rate. We, therefore, keep only this term and drop the amplitude in eq. (27).

To proceed further, we replace the operator $\vec{p}$ in the second matrix element in terms of the commutator of H_0 and $\vec{r}$ using eq. (22). We obtain

$$\langle f|T(t,t_0)|i\rangle = \frac{e^2\xi}{2\hbar V}\sqrt{\frac{1}{\omega_i\omega_f}}\int_{t_0}^{t} dt' e^{i(E_f - E_i - \hbar\omega_i + \hbar\omega_f)t'/\hbar}\mathcal{M}, \quad (30)$$

where

$$\mathcal{M} = \sum_n \frac{(E_f - E_n)}{E_n - E_i + \hbar\omega_f}\langle f|\vec{\epsilon}_\beta\cdot\vec{r}\,|n\rangle\mathcal{M}_{ni} \quad (31)$$

and

$$\mathcal{M}_{ni} = \langle n|\left[-\frac{1}{m_1}e^{i\vec{k}_f\cdot\vec{r}m_2/M} + \frac{1}{m_2}e^{-i\vec{k}_f\cdot\vec{r}m_1/M}\right]\vec{\epsilon}\,'_{\beta'}\cdot\vec{p}\,|i\rangle. \quad (32)$$

Using this, we obtain the transition rate as before,

$$\frac{d\tilde{P}}{dt} = \frac{1}{\Delta T}\int dE_{\gamma f}\rho_\gamma|\langle f|T(t_0,t)|i\rangle|^2, \quad (33)$$

where $E_{\gamma f} = \hbar\omega_f$ is the final-state photon energy and ρ_γ is the number density of photon states at energy $E_{\gamma f}$, given by eq. (18). In this case, the time integral will be proportional to $\Delta T\,\delta(E_f - E_i - \hbar\omega_i + \hbar\omega_f)$ where, as in the last section, $\Delta T = t - t_0$ is the total time. This transition rate corresponds to incident photon flux density of c/V. Hence, we should divide the rate by this flux density and multiply by the experimental flux density per unit frequency interval F_γ and integrate over frequency ω_i. We should also sum over the final photon polarisations and average over the initial photon polarisations. This leads to

$$\frac{dP}{dt} = \frac{1}{\Delta T}\int d\omega_i F_\gamma \frac{V}{c}\int dE'_\gamma \rho_\gamma|\langle f|T(t_0,t)|i\rangle|^2 = \frac{\alpha^2\xi^2}{c^2}\int d\omega_i F_\gamma \frac{\omega_f}{\omega_i}\frac{1}{2}\int d\Omega_f \sum_{\beta\beta'}|\mathcal{M}|^2, \quad (34)$$

where $\int d\Omega_f$ represents the integral over the directions of the emitted photon.

To obtain the cross-section, we take the initial and final states to be $S = 1/2, S_z = 1/2$ and $l = 0$. The intermediate state can take values $j = 3/2$ and $1/2$. We need to sum over all possible intermediate states, sum over

the photon polarisation vectors and perform the angular integration over the final-state photon momentum. The details of this calculation are presented in Appendix A where we compute the two matrix elements appearing in eq. (31). In the amplitude $\mathcal{M}_{ni}$ we expect that only one of the two terms will dominate. As we shall see, this depends on the nature of the wave function in the medium. Here, we assume that the term corresponding to m_2 in the exponent dominates. Here m_1 and m_2 represent the proton and the deuteron mass respectively. In eq. (31), $E_i \ll |E_f|, \hbar\omega_f \approx |E_f|$ and we shall be interested in E_n, such that $E_n \ll |E_f|$. Hence, we can set $|E_f - E_n| \approx E_n - E_i + \hbar\omega_f$.

Collecting all the factors, for the case of initial and final polarisation vectors $\vec{\epsilon}_1$ and $\vec{\epsilon}\,'_1$ respectively, we obtain using eq. (59)

$$\mathcal{M} = \frac{4\pi i \sin\phi_i}{m_1} \sum_n \int \mathrm{d}r' r'^2 R_f(r') r' R_n(r') \times \int \mathrm{d}r\, r^2 R_n(r) \frac{\sin k_1 r}{k_1^2 r^2} p_r R_i(r), \tag{35}$$

where R_i, R_n and R_f are the radial wave functions and $k_1 = m_2 k_f/(m_1 + m_2) \approx 2k_f/3$. Similarly, $\vec{\epsilon}_2$ and $\vec{\epsilon}\,'_1$ vectors lead to a similar result with $\cos\phi_i$ replaced by $\sin\phi_i$. Taking the absolute value squared of the two leads to a result independent of ϕ_i. The other two cases with $\vec{\epsilon}\,'_1$ replaced by $\vec{\epsilon}\,'_2$ yields a similar result for the absolute value squared with an overall factor of $\cos^2\theta_i$. We now need to integrate over the directions of the emitted photon. For this purpose, we change our coordinate system such that $\hat{z}$ is now aligned with the fixed vector $\hat{k}_i$. In this case, θ_i is replaced by the polar coordinate θ_f of the emitted photon. Integrating over solid angle ($\mathrm{d}\Omega_f$) and summing over all polarisation vectors, we obtain

$$\frac{1}{2}\int \mathrm{d}\Omega_f |\mathcal{M}|^2 = \frac{256\pi^3}{3m_1^2} \left| \sum_n \int \mathrm{d}r' r'^2 R_f(r') r' R_n(r') \times \int \mathrm{d}r\, r^2 R_n(r) \frac{\sin k_1 r}{k_1^2 r^2} p_r R_i(r) \right|^2. \tag{36}$$

Here we have also averaged over the initial photon polarisations.

The final result for reaction rate $\mathrm{d}P/\mathrm{d}t$ is obtained by substituting the angular integral in eq. (36) in eq. (34). In eq. (36), R_i, R_f and R_n are the radial wave functions. We express them as

$$R_i = \frac{u_i}{r} \tag{37}$$

with similar relationships for R_n and R_f. The wave function u_i is normalised to a plane wave and u_f is a bound-state wave function. In the case of u_n we need to sum over all energies E_n. This can be done by going to the continuum limit. In this case, the intermediate state wave function is normalised, such that,

$$\int_0^\infty \mathrm{d}r u(k') u(k) = \frac{\pi}{2}\delta(k - k'). \tag{38}$$

As we shall discuss later, we shall also consider a localised wave function for the intermediate state. Such wave functions can exist within a medium [45].

In the next section, we estimate the reaction rate for the process under consideration. Here we briefly discuss why we expect an enhancement in the second-order result at low energies. The basic observation is that the energy E_n can take any value. The tunnelling factor appears in eq. (36) in the nuclear matrix element, i.e., the integral over r'. The wave function R_n that appears in this integral corresponds to energy E_n rather than E_i. Since E_n can take a rather large value, the barrier tunnelling suppression factor may not be too small. However, there are potentially other suppression factors. The process is suppressed because it is a higher-order process and hence involves an additional power of α. We also expect that as E_n becomes large the amplitude will be suppressed since the intermediate state can only be short-lived. This suppression is essentially represented by the factor $(E_n - E_i + \hbar\omega_f)$ in the denominator in eq. (31). The molecular matrix element in eq. (36) is also significantly suppressed. In the limit of small k_1, the integral is expected to be very small since for large E_n, R_n will show very strong oscillations with r while the rest of the factors show a relatively slow change. For large k_1, the integral can be significant for $k_n \sim k_1$. In this case, we obtain a power suppression due to $1/k_1^2$ factor in the denominator. Furthermore, as we shall see, the sum over energies E_n also shows very delicate cancellations leading to a very small result as the upper limit on energy goes to infinity. Due to this suppression factor, the reaction rate turns out to be very small in free space. In medium, however, there can be special situations in which the process may lead to observable rates [45]. Finally, the reaction rate depends on the incident photon flux. As we have argued in [45], a related process in which two photons are spontaneously emitted tends to have a larger rate unless the incident photon flux is much larger than that is typically encountered in a laboratory.

4. Reaction rate

We first estimate the cross-section assuming free space. We directly solve the Schrödinger equation to obtain the wave functions u_i, u_n and u_f, using the potential given in eq. (10). We numerically estimate the integrals over r

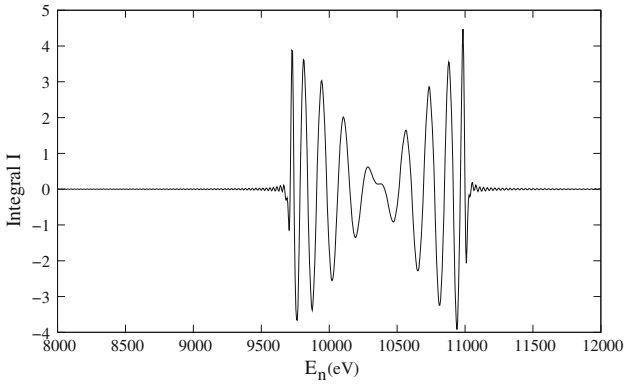

Figure 2. The integral I (in atomic units) defined in eq. (41) with the normalisation factors of u_i and u_n set to unity, as explained in the text.

and r'. For the integral over r, we impose an upper limit L. We assume $E_i \approx 10$ eV, and at large distances, u_i is given by

$$u_i(r) \to N \sin(k_i r + \phi_i), \tag{39}$$

where N is a normalisation factor. For the wave function u_n we use the continuum normalisation. In this case, the sum over n in eq. (36) is replaced by

$$\sum_n \to L \int \frac{\mathrm{d}k_n}{\pi} \tag{40}$$

with $L \to \infty$. In figure 2 we show the integral

$$I = \int_0^L \mathrm{d}r\, r\, u(n) \frac{\sin k_1 r}{r^2} \left(p_r \frac{u_i}{r}\right) \tag{41}$$

as a function of E_n. In this plot, we have set the normalisation factors of u_i and u_n equal to unity, i.e. at large distances these behave as $\sin(k_i r + \phi_i)$ and $\sin(k_n r + \phi_n)$ respectively. We see, as expected, that the integral is significant only for $k_n \sim k_1 = 2k_f/3$. As we move away from this region, the integral drops rapidly.

Using the integral I we can estimate the sum over energies and hence the cross-section. It turns out that sum over energies E_n, evaluated by using the continuum limit gives a rather small result [45], despite the fact that the tunnelling factor is not too small. We can understand this as follows. The integral I shows rapid oscillations with energy. In contrast, the nuclear matrix elements show relatively slow variation with energy. Hence, we expect that the integral of the product will be small. It can be sizeable only if I behaves as a delta function. Since for large distances, u_n and u_i show sinusoidal behaviour, we expect that I may show very sharp peaks at $k_n \sim k_1 \pm k_i$. However, this does not work since u_i shows sinusoidal behaviour only for $r > a_0$ where a_0 is the Bohr radius. For smaller r it decays very rapidly to zero. The calculation, therefore, fails to give an observable result in free space. This is, in fact, in agreement with experiments, where it is seen that the process works only in medium. Despite the fact that this leads to a small result, it would be interesting to make a precise estimate of it. This can be done by taking the integration limit over k_n to ∞. However, this calculation is rather difficult and we plan to do it as a future research.

In [45], we have argued that in medium the wave functions u_n can be modified to give an observable rate. One possibility is the presence of threshold effects. At some intermediate state energies, the proton–deuteron system would have enough energy to knock out an inner electron from the lattice atoms. At these energies, the eigenfunctions would show a sharp dependence on energy and the cancellation seen above may no longer be applicable. Another possibility is the toy model discussed in [45]. We argued that at large distances, the wave function may no longer display spherical symmetry. We assumed that the medium is such that the wave function has cylindrical symmetry at large distances. Furthermore, we assumed that for large ρ (in cylindrical coordinates) the potential is approximately zero and u_i and u_n behave as $\sin(k_n z + \phi_n)$ and $\sin(k_i z + \phi_i)$ respectively. This modification leads to observable reaction rates [45]. We may compare these proposed wave functions in the medium with the large distant free space wave functions, which behave as $\sin(kr + \phi)$, where r is the radial coordinate in spherical polar coordinates. The latter is spherically symmetric while the former has a wave vector pointing in some direction, which is taken to be z-axis. In the present paper, we consider another example of a medium wave function which may lead to observable rates.

4.1 *Localised states in the medium*

Let us start by assuming that the medium displays a periodic lattice structure. In that case, in analogy with electronic wave functions, we expect that proton and light nuclei will also show delocalised states which form bands. However, if the medium has sufficient impurities, then it will display localised states, analogous to Anderson localisation [54,55]. Such states are localised in space and would have widely separated energy eigenvalues. We next assume that one such state exists in the energy regime where the integral I, shown in figure 2, is significant. Then it is clear that we shall obtain a larger contribution to the reaction rate.

We do not pursue a detailed study of localised states in the present paper. However, we briefly elaborate on them by considering a one-dimensional model. Consider a deuteron–hydrogen system in a disordered system. So, besides the two-body Coulomb repulsion, these particles would also experience Coulomb repulsion due to lattice ions, as shown in the one-dimensional model in figure 3.

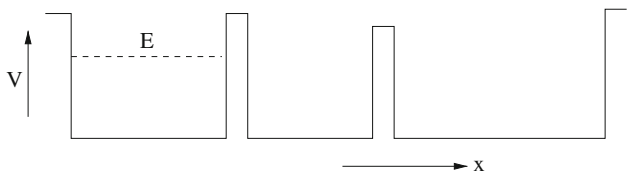

Figure 3. A representative one-dimensional potential for a random medium. The widths and heights of the potential wells change randomly with position.

The particle essentially experiences a random potential in which the width and height of the potential wells is not uniform. We assume that E is less than the top of the potential steps, as shown in figure 3. In the region where the potential is zero, the wave function would show an oscillatory behaviour. In the potential step region, it will have exponentially decaying and growing solutions. An eigenfunction which is delocalised over large distances in the medium with approximately uniform amplitude is highly unlikely. This is because it would have to simultaneously satisfy appropriate boundary conditions at each step which would become nearly impossible as the number of steps increases. We may, however, find spatially localised states. For any region of space, such states would behave as bound states and would have widely separated energies. Here we assume that one such state exists in the spatial region in which the deuteron–hydrogen system is located in the energy range of 1–10 keV. If such a state exists, then we can just use this state to estimate the rate and ignore all the delocalised states because the amplitude of this state would be very different from all the remaining states and, hence, we do not expect the cancellation that we found earlier would arise in this case leading to an enhanced rate.

In application to our three dimensional system, we point out that it is not necessary that the wave function has to be localised in all directions. For example, we may consider particles incident on a surface, which have delocalized wave functions in the outer hemisphere but may be localised in the hemisphere towards the surface. This would also lead to widely separated energy eigenvalues which may lead to a significant reaction rate.

We essentially visualise the lattice to form a three-dimensional trap for the nuclear system. At each lattice site, the boundary condition has to be such that the wave function must decay. We assume a palladium lattice with $Z_{\rm P} = 46$ and density $\rho = 11.9$ gm/cm^3. We find that the number density of palladium atoms is $n = 0.01$ in atomic units. Each lattice atom would present a potential barrier over a solid angle $\pi r^2/R^2$ where R is the distance of the atom from the centre of mass of the deuteron–hydrogen system and r is the turning point. We obtain r by setting $E = V = Z_P/r$. The wave function must decay exponentially over the solid angle $\pi r^2/R^2$. By continuity, the decay may be applicable over a solid angle much larger than this. For a simple estimate, we assume that the wave function decays strongly over a radius roughly $2r$ and hence solid angle $4\pi r^2/R^2$. We next determine the length scale L over which the total solid angle due to all lattice sites is 4π. It is clear that over this distance, the particle will hit a potential barrier in all directions. Hence, this provides an estimate of the distance scale over which we may assume the existence of a localised state for such high energies. Integrating over the solid angle,

$$\int_{4\pi} {\rm d}\Omega = \int_0^L \left(\frac{4\pi r^2}{R^2}\right) n 4\pi R^2 {\rm d}R, \tag{42}$$

for E in the range 1–10 keV. This leads to $L \approx 5$–500 in atomic units. Essentially, the lattice acts as a three-dimensional potential barrier of mean radius L.

4.2 *Reaction rate estimate*

We next compute the reaction rate per particle, assuming that the incident state is also a localised state within the medium. As mentioned earlier, the energy eigenvalue of this state is taken to be 10 eV. We assume that it displays sinusoidal behaviour, shown in eq. (39), over some distance and then decays rapidly at larger distances. To compute the reaction rate, we set the incident photon flux equal to 10^{20} per cm^2 per second at visible frequencies. Such a flux may be applicable for a laser. For $E_n \approx 10$ keV we find reaction rate of order 10^{-38} per second. In computing this, an important factor is the nuclear matrix element, i.e. the integral over r' in eq. (36). This is found to be about 3×10^{-10} with the normalisation of R_n set to unity. This means that at distances larger than the nuclear length scales, $R_n \sim \sin(k_n r)/r$. The result actually has a relatively mild dependence on E_n over the range of about 3–10 keV but falls very rapidly as we go to lower energies. The reaction rate may be several orders of magnitude smaller than our estimate due to the shielding effect of the electronic cloud [56].

The reaction rate obtained above is much larger than what would be achieved for the standard fusion reaction given in eq. (2). As discussed later, the two-photon emission process also leads to a much larger rate. For our choice of screening potential ($r_0 = 1$ Bohr radius), we obtain a reaction rate of order 10^{-73}/s . This gets enhanced to 10^{-61}/s if $r_0 = 1/1.9$ Bohr radius. Hence, this is very sensitive to the screening potential but appears to be very small for all reasonable choices of screening potential. We point out that the rate for the second-order process is not very sensitive to the

choice of screening potential. It is clear that the proposed mechanism has the potential to lead to significant enhancement. However, the reaction rate, even for the photon absorption mechanism, is found to be quite small and cannot be observed. In contrast, the emission process considered in [45] leads to a rate of about 10^{-16}/s in special medium conditions, which is also small but observable. This process is not affected by the electron shielding effect discussed in [56]. One of the difference in the two calculations is that in [45] we used the magnetic moment term in the interaction Hamiltonian shown in eq. (12). This leads to a significant enhancement mainly because of the absence of k_1^2 term in the denominator in eq. (36). This leads to an enhancement factor of $k_1^4 \sim 10^{12}$ for our choice of parameters. Furthermore, the incident photon flux, even for a laser, is not too strong and the spontaneous emission mechanism generically produces a larger reaction rate.

4.3 *Reaction rate: Two-photon emission*

In §4.2, we have estimated the reaction rate for the nuclear fusion process induced by an incident flux of photons (eq. (1)). We have found that the reaction rate in a medium can be considerably larger than the rate in free space. However, the rate turns out to be relatively small and not observable. Based on the results of [45], we expect that the rate may be larger if we consider the magnetic moment interaction term in eq. (12). However, it is still expected to be smaller than the rate of the associated process of emission of two photons discussed in detail in [45], which may lead to observable rates in the medium. In this section, we use the proposed localised wave function, discussed above, and the results of [45] to compute the rate of the two-photon emission process.

In [45], the incident and final eigenfunctions were taken to be $l = 0, s = 1/2$ states with intermediate state being $l = 1$. The first perturbation was taken to be the magnetic moment interaction, i.e. the third term on the right-hand side of eq. (12). Hence, at this vertex, the process follows the selection rules of magnetic transitions and is forbidden at leading order. It can proceed only if the photon has non-zero orbital angular momentum. The standard expectation is that such processes are suppressed. However, in the present case, the relevant value of the radial coordinate is large and the standard rules are not applicable. In fact, in analogy with the process in eq. (1), the process with two photons in the final state is also heavily suppressed in free space. This suppression does not arise due to spin-parity selection rules, but rather due to a delicate cancellation as we sum over all eigenstates in the intermediate state $|n\rangle$ (see eq. (28)). However, as explained earlier, in the medium the rate may be large.

In our calculation, we include only the contribution due to proton in eq. (12) and drop that of deuteron, as the latter is expected to be much smaller. A high-energy photon gets emitted and we need to include the full spatial dependence of the photon as in the calculation in §3. The second perturbation is taken to be the first two terms on the right-hand side of eq. (12) and leads to the emission of another high-energy photon. The details are presented in [45]. Let the radial wave function for the initial, intermediate and final states be, $R_i = u_i(r)/r$, $R_n = u_n(r)/r$ and $R_f = u_f(r)/r$. Let $E_1 = \hbar\omega_1$ and $E_2 = \hbar\omega_2$ be the energies of the photons emitted due to the first and second perturbations respectively. The wave numbers of these two photons are k_1 and k_2 respectively. The final result for the reaction rate is given by [45]

$$\frac{\mathrm{d}P}{\mathrm{d}t} = \frac{\alpha^2\xi^2 g_p^2}{2\pi\hbar^2 c^6 m_p^2}\int \mathrm{d}E_1 E_1^3 E_3 |I|^2, \tag{43}$$

where

$$I = \sum_n I_1 I_2 \frac{E_f - E_n}{E_n - E_i + E_1}, \tag{44}$$

$$I_1 = \int_0^\infty \mathrm{d}r u_n^* \frac{\cos\tilde{k}_1 r}{\tilde{k}_1 r} u_i, \tag{45}$$

$$I_2 = \int_0^\infty \mathrm{d}r' u_f^* r' u_i \tag{46}$$

and $\tilde{k}_1 = k_1 m_2/(m_1 + m_2) \approx 2k_1/3$.

In the present case, we only have one term contributing to the sum over n in eq. (44). This is the localised state whose energy eigenvalue E_{loc} may be treated as a free parameter. We expect significant contribution for E_{loc} in the range of about 1–9 keV. For values of E_{loc} larger than approximately 11 keV the corresponding wave number exceeds that of the emitted photon and hence the contribution would be negligible. For $E_{\mathrm{loc}} < 1$ keV, the barrier penetration would lead to a strong suppression. We point out that the total two-photon energy $E_1 + E_2 < Q$, where $Q \approx 5.49$ MeV is the Q value of the process. We perform the calculation of the reaction rate by assuming that the initial state is the ground state of hydrogen and deuteron with energy eigenvalue -4.68 eV [45]. We compute this eigenfunction by choosing an appropriate molecular potential [45]. For $E_{\mathrm{loc}} = 8$ keV, the energy dependence of the differential rate $\mathrm{d}P/(\mathrm{d}t\,\mathrm{d}E_1)$ is shown in figure 4. The dependence of the rate $\mathrm{d}P/\mathrm{d}t$ on the parameter E_{loc} is shown in figure 5. We find that the maximum value of the rate is about 5.7×10^{-16} s^{-1} for $E_{\mathrm{loc}} \approx 6$ keV. This is of the same order as that found using a different model for medium wave function in [45]. It comes down to about 4.8×10^{-19} s^{-1} for $E_{\mathrm{loc}} = 1$ keV and falls very sharply for smaller values of this parameter.

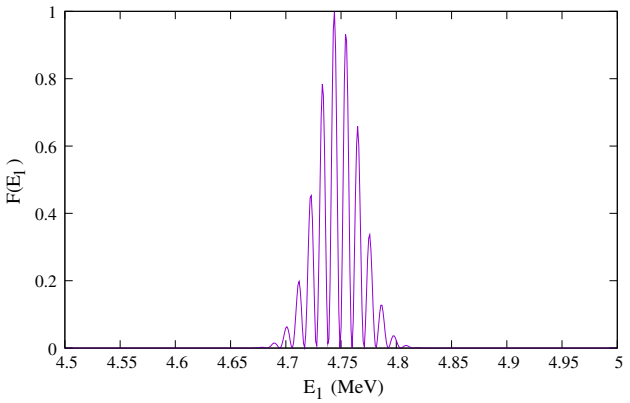

Figure 4. The differential reaction rate $F(E_1) = \mathrm{d}P/(\mathrm{d}t\,\mathrm{d}E_1)$ as a function of the photon energy E_1 for the parameter $E_{\mathrm{loc}} = 8$ keV. Here the rate has been normalised so that the maximum value is unity.

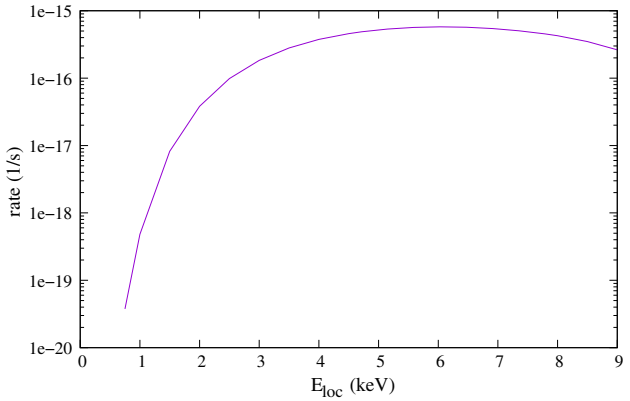

Figure 5. The reaction rate $\mathrm{d}P/\mathrm{d}t$ (s^{-1}) as a function of the energy eigenvalue E_{loc} of the localised state.

The rate also falls sharply for E_{loc} greater than 9 keV. The rate is small but observable over this entire range.

4.4 *Experimental signature*

As we have shown in §4.3, given a suitable medium wave function, the two-photon emission process leads to observable rates. Let us consider the rate 4.8×10^{-19} s^{-1} when $E_{\mathrm{loc}} = 1$ keV. We may assume hydrogen concentration to be $10^{23}/\mathrm{cm}^3$. Assuming the natural isotopic ratio, this implies a concentration of about 10^{19} deuterons/cm^3. Hence, for typical experimental conditions, we expect a few reactions per minute and may get observable signal within a reasonable observation time. The success of the experiment depends on the sample size which has been properly loaded with hydrogen and deuteron. The process leads to the emission of two photons in coincidence with their total energy roughly equal to the Q value (5.49 MeV) of the process. The precise value can be computed by accounting for the nuclear recoil and energy loss of photons as they emerge from the medium. Hence, it produces a clean signal which can be tested experimentally. For a particular value of the parameter E_{loc} each of the two photons would also have energy in a very narrow range. Hence, for example, for $E_{\mathrm{loc}} = 8$ keV we expect one photon at energy around 4.75 MeV (see figure 4) and the other photon at roughly 700 keV. However, this parameter may vary with position in the medium and we may not get photons at precisely these energy values. However, the sum of the two-photon energy must be of the order of the Q value of the process. The process does require a special wave function in a medium, which might explain why it is not observed in all experiments. Here and in [45] we have provided some examples of medium wave function which can lead to observable rates. However, a detailed analysis of such wave functions is needed, which is so far lacking in the literature.

5. Discussion and conclusions

We have introduced a new mechanism for nuclear fusion which may play an important role at low energies. We propose that the reaction takes place by an electromagnetic perturbation. In most of our analysis, we have assumed that this perturbation is caused by an incident flux of real photons. The fusion reaction then proceeds by forming a virtual state whose energy is unrestricted and we need to consider contributions from all energies. Due to the high energy possible for these states, the barrier penetration probability is not very small and it does not lead to a strong suppression of the cross-section. The dominant suppression in the current case arises from the incident flux factor of photons or other particles, the use of relatively high-energy intermediate states and the fact that the process involves second-order in perturbation theory. The barrier penetration factor also leads to a suppression but it is much milder than the standard process.

We have performed a detailed calculation of the hydrogen and deuteron fusion reaction to form helium with $A = 3$. In free space, the reaction rate is found to be rather small. The calculation is rather tricky in this case, since we need to integrate over infinite range of intermediate state energies. However, it is clear that the rate is relatively small and not very interesting. In a medium, we find that there can be special situations which can lead to significant enhancement. These have been discussed in detail in a follow up paper [45]. In the present paper, we considered a particular situation involving localised states in a medium. Such states are analogous to the phenomenon of Anderson localisation but in the present case applied to the deuteron–hydrogen

system in a medium. We argued that the potential offered by the medium leads to the existence of localised states. The length scale of localisation for the energies relevant to our process may be of the order of 5–500 Bohr radius, depending on energy eigenvalue of the state. However, the main point is that such states are also localised in energy and we can estimate the reaction rate considering only one such state, while ignoring other states which extend throughout the medium. Such localised states lead to a reaction rate much larger than the rate of the standard fusion process for the same incident energy. However, even with such enhancement, the reaction induced by incident photon flux is found to be quite small and not observable.

In [45] we have also considered another reaction which involves emission of two photons, without requiring an incident flux of photons. The rate for this reaction is found to be much larger. This arises partially due to the fact that we used the magnetic moment interaction terms in the Hamiltonian, given in eq. (12). This term leads to a significantly larger rate than to what is obtained by the first two terms on the right-hand side of eq. (12). Furthermore, for most photon flux values achieved in laboratory, the two-photon emission process generically leads to a larger rate. We have computed the rate for the two-photon emission process using our localised wave function model. We find that this leads to observable rates for a wide range of the values of the energy eigenvalue ($E_{\rm loc}$) of the localised state.

The emission process [45] also leads to a very clean signal of the proposed mechanism involving second-order perturbation theory. It predicts emission of two photons in coincidence, with combined energy equal to approximately the Q value of the process, which is about 5.49 MeV. We look forward to an experimental test of our proposal, which may confirm or rule out our proposed mechanism for low energy nuclear reactions.

Acknowledgements

The authors are very grateful to Mahadeva Srinivasan, Manoj Harbola, Amit Agarwal and Aditya Kelkar for useful discussions.

Appendix

In this appendix, we provide details of the angular integrals in the sum over energies in the intermediate state. We consider the initial state with $S = 1/2$, $S_z = 1/2$ and $l = 0$. The intermediate state has $l = 1$. With $S = 1/2$ and $l = 1$ we can form two states with $j = 3/2$ and $j = 1/2$. The states $|j, j_z\rangle$ that are relevant for us are

$$\begin{aligned}
|3/2, 3/2\rangle &= |1/2, 1/2; 1, 1\rangle,\\
|3/2, -1/2\rangle &= \sqrt{1/3}\,|1/2, 1/2; 1, -1\rangle\\
&\quad +\sqrt{2/3}\,|1/2, -1/2; 1, 0\rangle,\\
|1/2, -1/2\rangle &= -\sqrt{2/3}\,|1/2, 1/2; 1, -1\rangle\\
&\quad +\sqrt{1/3}\,|1/2, -1/2; 1, 0\rangle,
\end{aligned} \tag{47}$$

where on the right-hand side the states are shown in notation $|S, S_z; l, l_z\rangle$. Let us take the final photon direction to be along the z-axis, i.e. $\hat{k}_f = \hat{z}$. The corresponding polarisation vectors are along the $\hat{x}$- and $\hat{y}$-axes. Let us consider any one of the amplitudes appearing in eq. (32),

$$\mathcal{M}_1 = \langle n|e^{i\vec{k}_1\cdot\vec{r}}\vec{\epsilon}\,'_{\beta'}\cdot\vec{p}|i\rangle. \tag{48}$$

Since the initial state has $l = 0$, we can express this as

$$\mathcal{M}_1 \equiv \int d^3r\,\psi_n^* e^{i\vec{k}_1\cdot\vec{r}}\vec{\epsilon}\,'_{\beta'}\cdot\hat{r}\,p_r\psi_i. \tag{49}$$

We have $\vec{\epsilon}\,'_1\cdot\hat{r} = \sin\theta\cos\phi$ and $\vec{\epsilon}\,'_2\cdot\hat{r} = \sin\theta\sin\phi$. The intermediate wave function ψ_n corresponds to $l = 1$. We get non-zero contributions only for $\psi_n \sim Y_1^1$ and $\psi_n \sim Y_1^{-1}$. Hence, we have four relevant combinations involving the two polarisation vectors and the two spherical harmonics. Let us consider one of these angular integrals, given by

$$\begin{aligned}
I_1 &\equiv \int d\Omega Y_1^{1*}(\hat{r})e^{i\vec{k}_1\cdot\vec{r}}\vec{\epsilon}\,'_1\cdot\hat{r}\\
&= -\frac{1}{2}\sqrt{\frac{3}{2\pi}}\int d\Omega\sin\theta e^{-i\phi}e^{ik_1r\cos\theta}\sin\theta\cos\phi.
\end{aligned} \tag{50}$$

In performing the integral over the polar angle θ we keep only the leading-order contribution. We obtain

$$I_1 = \left(\frac{1}{2}\sqrt{\frac{3}{2\pi}}\right)4\pi i\,\frac{\sin k_1r}{k_1^2r^2}. \tag{51}$$

Here we have dropped terms of higher order in $1/k_1r$, which will be small since k_1 takes rather large values. Similarly, we have the remaining integrals

$$I_2 \equiv \int d\Omega Y_1^{1*}(\hat{r})e^{i\vec{k}_1\cdot\vec{r}}\vec{\epsilon}\,'_2\cdot\hat{r} = -iI_1 \tag{52}$$

$$I_3 \equiv \int d\Omega Y_1^{-1*}(\hat{r})e^{i\vec{k}_1\cdot\vec{r}}\vec{\epsilon}\,'_1\cdot\hat{r} = -I_1 \tag{53}$$

and

$$I_4 \equiv \int d\Omega Y_1^{-1*}(\hat{r})e^{i\vec{k}_1\cdot\vec{r}}\vec{\epsilon}\,'_2\cdot\hat{r} = -iI_1. \tag{54}$$

We next consider the final-state matrix element

$$\mathcal{M}_2 \equiv \langle f|\vec{\epsilon}\cdot\hat{r}|n\rangle. \tag{55}$$

Let the initial photon momentum be

$$\vec{k}_i = k_i \left[\sin\theta_i(\cos\phi_i\hat{x} + \sin\phi_i\hat{y}) + \cos\theta_i\hat{z}\right]. \quad (56)$$

The corresponding polarisation vectors can then be taken as

$$\vec{\epsilon}_1 = \sin\phi_i\hat{x} - \cos\phi_i\hat{y}$$

$$\vec{\epsilon}_2 = \cos\theta_i(\cos\phi_i\hat{x} + \sin\phi_i\hat{y}) - \sin\theta_i\hat{z}. \quad (57)$$

By a suitable choice of coordinates, we can set $\phi_i = 0$. In any case, it will cancel out in the final result. We again find four relevant angular integrals in $\mathcal{M}_2$. These are

$$I_1' \equiv \int d\Omega'\, \vec{\epsilon}_1 \cdot \hat{r}'\, Y_1^1(\hat{r}') = \left(\frac{1}{2}\sqrt{\frac{3}{2\pi}}\right)\frac{4\pi}{3} i e^{i\phi_i}$$

$$I_2' \equiv \int d\Omega'\, \vec{\epsilon}_1 \cdot \hat{r}'\, Y_1^{-1}(\hat{r}') = -I_1'^*$$

$$I_3' \equiv \int d\Omega'\, \vec{\epsilon}_2 \cdot \hat{r}'\, Y_1^1(\hat{r}') = i\cos\theta_i I_1'$$

$$I_4' \equiv \int d\Omega'\, \vec{\epsilon}_2 \cdot \hat{r}'\, Y_1^{-1}(\hat{r}') = i\cos\theta_i I_1'^*. \quad (58)$$

Let us now consider the case in which the initial and final polarizstion vectors are $\vec{\epsilon}_1$ and $\vec{\epsilon}\,'_1$. In this case, adding contributions from all the states in eq. (47), we obtain

$$\mathcal{M}_2\mathcal{M}_1 = -4\pi i \sin\phi_i \int dr' r'^2 R_f(r') r' R_n(r')$$

$$\int dr\, r^2 R_n(r) \frac{\sin k_1 r}{k_1^2 r^2} p_r R_i(r), \quad (59)$$

where R_i, R_n and R_f are the radial wave functions.

References

[1] M Fleischmann and S Pons, *J. Electroanal. Chem. Interf. Electrochem.* **261**, 301 (1989)
[2] S E Jones *et al*, *Nature* **338**, 737 (1989)
[3] S E Koonin and M Nauenberg, *Nature* **339**, 690 (1989)
[4] A J Leggett and G Baym, *Phys. Rev. Lett.* **63**, 191 (1989)
[5] S B Krivit, *Nuclear energy encyclopedia* (John Wiley & Sons, Ltd., 2011), Ch. 41, p. 479
[6] L I Urutskoev, *Nuclear energy encyclopedia* (John Wiley & Sons, Ltd., 2011), Ch. 42, p. 497
[7] M Srinivasan, G Miley and E Storms, *Nuclear energy encyclopedia* (John Wiley & Sons, Ltd., 2011), Ch. 43, p. 503
[8] J M Zawodny and S B Krivit, *Nuclear energy encyclopedia* (John Wiley & Sons, Ltd., 2011), Ch. 44, p. 541
[9] W Williams and J Zawodny, *Nuclear energy encyclopedia* (John Wiley & Sons, Ltd., 2011), Ch. 45, p. 547
[10] A Meulenberg, *Curr. Sci.* **108**, 499 (2015)
[11] A Takahashi, *Curr. Sci.* **108**, 514 (2015)
[12] K P Sinha, *Curr. Sci.* **108**, 516 (2015)
[13] C L Liang, Z M Dong and X Z Li, *Curr. Sci.* **108**, 519 (2015)
[14] E Storms, *Curr. Sci.* **108**, 535 (2015)
[15] M C McKubre, *Curr. Sci.* **108**, 495 (2015)
[16] J-P Biberian, *Curr. Sci.* **108**, 633 (2015)
[17] M Srinivasan and K Rajeev, *Cold fusion* (Elsevier, 2020), Ch. 13, p. 233
[18] J-P Biberian, *Cold fusion: Advances in condensed matter nuclear science* (Elsevier, 2020)
[19] A Huke, K Czerski, P Heide, G Ruprecht, N Targosz and W Żebrowski, *Phys. Rev. C* **78**, 015803 (2008)
[20] V Pines *et al*, *Phys. Rev. C* **101**, 044609 (2020)
[21] V Vysotskii and M Vysotskyy, *EPJA* **49**, 08 (2013)
[22] S Bartalucci, V I Vysotskii and M V Vysotskyy, *Phys. Rev. Accel. Beams* **22**, 054503 (2019)
[23] C Spitaleri, C Bertulani, L Fortunato and A Vitturi, *Phys. Lett. B* **755**, 275 (2016)
[24] P Kálmán and T Keszthelyi, *Phys. Rev. C* **99**, 054620 (2019)
[25] P Hagelstein, *JCMNS* **16**, 46 (2015)
[26] A Widom and L Larsen, *EPJC* **46**, 107 (2006)
[27] Y Srivastava, A Widom and L Larsen, *Pramana – J. Phys.* **75**, 617 (2010)
[28] J-L Paillet and A Meulenberg, *JCMNS* **29**, 472 (2019)
[29] H Assenbaum, K Langanke and C Rolfs, *Z. Phys. A: Atomic Nuclei* **327**, 461 (1987)
[30] S Ichimaru, *Rev. Mod. Phys.* **65**, 255 (1993)
[31] V A Chechin, V A Tsarev, M Rabinowitz and Y E Kim, *Int. J. Theor. Phys.* **33**, 617 (1994)
[32] J Kasagi, H Yuki, T Baba, T Noda, T Ohtsuki and A G Lipson, *J. Phys. Soc. Jpn* **71**, 2881 (2002)
[33] F Raiola *et al*, *EPJA* **19**, 283 (2004)
[34] K Czerski, A Huke, P Heide and G Ruprecht, *The 2nd International Conference on Nuclear Physics in Astrophysics* (Springer, 2006), p. 83
[35] M Coraddu, M Lissia and P Quarati, *Cent. Eur. J. Phys.* **7**, 527 (2009)
[36] K Czerski *et al*, *EPL* **113**, 22001 (2016)
[37] T Schenkel *et al*, *J. Appl. Phys.* **126**, 203302 (2019)
[38] C Berlinguette *et al*, *Nature* **570**, 45 (2019)
[39] S Focardi *et al*, *Condensed matter nuclear science* (World Scientific, 2006), p. 70
[40] E Storms and B Scanlan, *JCMNS* **11**, 142 (2013)
[41] L Holmlid and S Olafsson, *Int. J. Hydrogen Energy* **40**, 10559 (2015)
[42] M Srinivasan, *JCMNS* **15**, 137 (2015)
[43] N Packham *et al*, *J. Electroanal. Chem.* **270**, 451 (1989)
[44] E Merzbacher, *Quantum mechanics* (Wiley, 1998)
[45] P Jain *et al*, *JCMNS* **35**, 1 (2022)
[46] D D Clayton, *Principles of stellar evolution and nucleosynthesis* (The University of Chicago Press, Chicago, 1968)
[47] C A Bertulani, *Nuclear physics in a nutshell* (Princeton University Press, 2007)
[48] H-S Bosch and G Hale, *Nucl. Fusion* **32**, 611 (1992)

[49] C A Bertulani and T Kajino, *Prog. Part. Nucl. Phys.* **89**, 56 (2016)
[50] P Jain, *An introduction to astronomy and astrophysics* (CRC Press, 2016)
[51] J J Sakurai, *Advanced quantum mechanics* (Pearson Education, 1967)
[52] A Dodonov and V Dodonov, *Phys. Lett. A* **378**, 1071 (2014)
[53] K P Rajeev and D Gaur, *JCMNS* **24**, 278 (2017)
[54] E Abrahams, *50 Years of Anderson localization* (World Scientific, 2010)
[55] P A Lee and T V Ramakrishnan, *Rev. Mod. Phys.* **57**, 287 (1985)
[56] J I Gersten and M H Mittleman, *Phys. Rev. Lett.* **48**, 651 (1982)